possible point 6 can make them more probable than the sequences retained. The *b* sequence is now more probable. In step 5, when point 6 is known, only the *b* sequence is retained.

If the elements h_{ij} have different probabilities apart from continuity considerations (which will normally be the case, if they have initially been found by some such method as isomorphous replacement), these initial probabilities can be included at both the sequence-extension stage and the final selection stage.

References

BARRETT, A. N., BARRINGTON LEIGH, J., HOLMES, K. C., LEBERMAN, R., MANDELKOW, E., VON SENGBUSCH, P. & KLUG, A. (1971). *Cold Spring Harbour Symp. Quant. Biol.* **36**, 433–448.

BRAGG, W. L. & PERUTZ, M. F. (1952). *Proc. Roy. Soc.* A**213**, 425–435.

CASPAR, D. L. D. (1956). *Nature, Lond.* **177**, 928.

COCHRAN, W., CRICK, F. H. C. & VAND, V. (1952). *Acta Cryst.* **5**, 581–586.

FINCH, J. T. (1965). *J. Mol. Biol.* **12**, 612–619.

FRANKLIN, R. E. (1956). *Nature, Lond.* **177**, 928–930.

FRANKLIN, R. E. & KLUG, A. (1955). *Acta Cryst.* **8**, 777–780.

HOLMES, K. C. (1959). *X-ray Diffraction Studies on Tobacco Mosaic Virus and Related Substances.* Thesis, Univ. of London.

HOLMES, K. C., STUBBS, G. J., MANDELKOW, E. & GALLWITZ, U. (1975). *Nature, Lond.* **254**, 192–196.

KLUG, A., CRICK, F. H. C. & WYCKOFF, H. W. (1958). *Acta Cryst.* **11**, 199–213.

KRAUT, J., SIEKER, L. C., HIGH, D. F. & FREER, S. T. (1962). *Proc. Natl. Acad. Sci. U.S.* **48**, 1417–1424.

ROLLETT, J. S. (1965). *Computing Methods in Crystallography.* Oxford: Pergamon Press.

STUBBS, G. J. (1972). *Structural Studies of Crystalline Proteins.* Thesis, Univ. of Oxford.

WASER, J. (1955). *Acta Cryst.* **8**, 142–150.

Acta Cryst. (1975). A**31**, 718

Self-Crystallizing Molecular Models. IV. Revision and Conclusion

BY TARO KIHARA

Department of Physics, Faculty of Science, University of Tokyo, Tokyo, Japan

(*Received* 31 *March* 1975; *accepted* 23 *April* 1975)

Molecular models with magnetic multipoles, which were invented by the author for the purpose of simulating crystal structures, are revised. The models of the new type are made of Ba ferrite magnets and plastic pieces only, no Mn–Zn ferrite being used. The crystal structures of SiF_4 and α-CF_4, as well as those of UCl_6 and WCl_6 are represented by use of different species of molecular models.

Introduction

The purpose of this series of papers (Kihara, 1963, 1966, 1970) is to explain the structures of molecular crystals in terms of the shapes of the molecules as well as the intermolecular force. We treat rigid nonpolar molecules with no power to form hydrogen bonds.

If the molecules do not possess any appreciable electric multipoles, the crystal structures are governed by the principle of closest packing of the molecules. The orthorhombic crystals of Cl_2, Br_2 and I_2, and the cubic crystals of SiI_4, GeI_4, SnI_4, *etc.* are examples of such structures.

If, on the other hand, the molecules have sufficiently strong electric multipoles, the electrostatic interaction often governs the crystal structure. In such cases, the crystal structure does not necessarily correspond to the closest packing of the molecules.

The electrostatic multipolar interaction between molecules can be represented by use of molecular models with magnetic multipoles. A structure into which these models are assembled will simulate the actual crystal structure.

In Part II (1966), eight types of molecular models made of barium ferrite magnets were given. In Part III (1970), models consisting of barium ferrite magnets

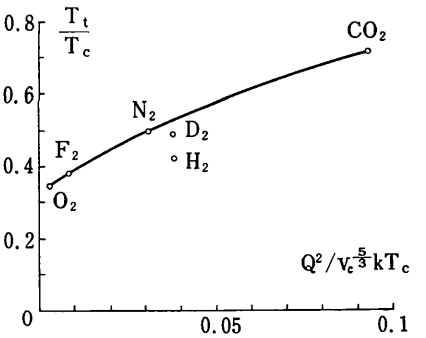

Fig. 1. Ratio of the triple-point to the critical-point temperatures as a function of the dimensionless quadrupolar interaction.

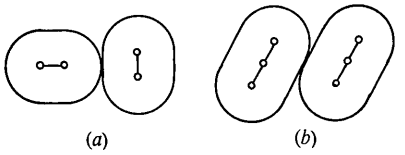

Fig. 2. Relative orientations with minimum potential energy for D_2 and N_2 (*a*), and for CO_2 (*b*).

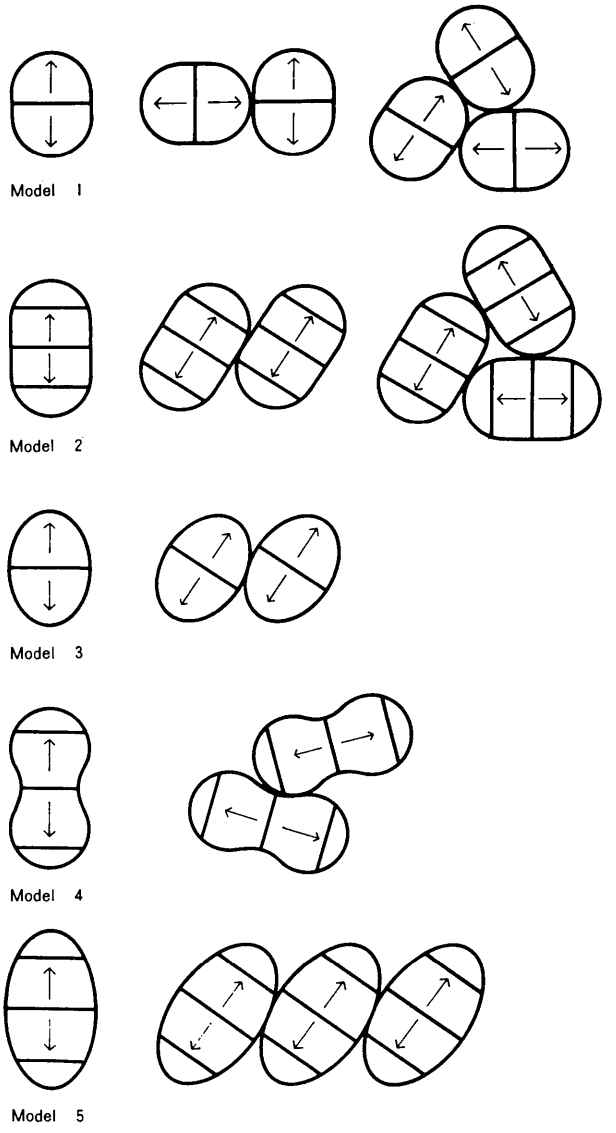

Fig. 3. Models of rod-like quadrupolar molecules and their minimum-energy configurations. The parts with arrows are Ba-ferrite magnets; those without arrows are plastic pieces. Model 1 is for D_2 and N_2; Model 2 is for CO_2; Model 3 is for acetylene HCCH; Model 4 is for cyanogen NCCN; Model 5 is for $ClCH_2CH_2Cl$ and

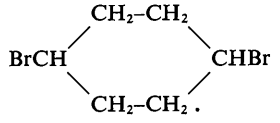

and manganese zinc ferrite pieces were included. There, the manganese zinc ferrite, whose permeability is greater than 1000, was considered to play the role of the polarizability of a molecule in the field of adjacent molecules. The present paper makes a thorough revision of Part III with respect to these 'polarizable' models.

The revision is based on the fact that the force due to the polarization of a molecule induced in the field of the permanent multipoles of adjacent molecules is usually negligible as compared with the direct electrostatic forces between multipoles. Instead of the material with large permeability, we use in the present paper non-magnetic material (plastic or wood). Thus the models given in the following are simpler but nevertheless more realistic than the polarizable models in Part III.

Multipole interactions in solids

In the gaseous and liquid states, electric multipolar interactions between nonpolar molecules are negligible. In the solid state, however, these interactions play an important role.

Let us first consider the ratio T_t/T_c, T_t and T_c being the temperature at the triple point and the temperature at the gas–liquid critical point, respectively. This ratio is 0·55 for Ne, Ar, Kr and Xe. For symmetric linear molecules, the ratio takes the values in the following sequence: carbon disulphide CS_2, 0·29; oxygen O_2, 0·35; fluorine F_2, 0·37; chlorine Cl_2, 0·41; hydrogen H_2, 0·42; deuterium D_2, 0·49; nitrogen N_2, 0·50; cyanogen $(CN)_2$, 0·61; acetylene C_2H_2, 0·62 and carbon dioxide CO_2, 0·71. Since the shapes of these molecules are similar, these values indicate how much the depth of the intermolecular potential depends on the relative orientations of the molecules.

In order to show that the quadrupolar interaction plays an essential part in this dependence of the potential depth on the molecular orientations, we calculate the dimensionless quantity $Q^2v_c^{-5/3}(kT_c)^{-1}$. Here v_c is the volume per molecule at the critical point, k is the Boltzmann constant, and Q is the quadrupole moment. The values of this quantity for

$$O_2,\ F_2,\ N_2,\ D_2,\ CO_2$$

are in the proportion

$$0{\cdot}02:0{\cdot}08:0{\cdot}28:0{\cdot}37:1{\cdot}00.$$

Fig. 1 shows clearly the importance of the electrostatic multipolar interactions in solids. Molecular models of the present type apply to CO_2, C_2H_2, $(CN)_2$, N_2 and D_2 but not to F_2, O_2 or CS_2.

The ratio T_t/T_c is 0·39 for carbon tetrafluoride CF_4 and 0·73 for silicon tetrafluoride SiF_4, indicating large octopolar interaction for SiF_4. In fact, the crystal structure of CF_4 is different from that of SiF_4.

Crystals which are additionally stabilized by large

multipoles of the molecules often do not melt but sublimate under atmospheric pressure. Thus, solid carbon dioxide sublimates at −78·5°C, acetylene −84°C, silicon tetrafluoride −95°C, sulphur hexafluoride SF_6 −63°C, uranium hexafluoride UF_6 56·5°C, and hexamethylenetetramine $(CH_2)_6N_4$ 263 °C.

Quadrupolar molecules

The intermolecular potentials for D_2, N_2, O_2, F_2 and CO_2 were recently calculated as functions of the distance between the molecular centres and the relative orientations of the two molecules (Koide & Kihara, 1974). For D_2 and N_2, the relative orientation shown in Fig. 2(*a*) corresponds to the minimum potential energy; for CO_2, the minimum-energy orientation is as shown in Fig. 2(*b*).

Model 1 for D_2 or N_2 and Model 2 for CO_2 in Fig. 3 have such characteristics. An assembly of these molecular models simulates a cubic crystal structure with the space group $Pa3$, to which solid carbon dioxide and the lowest-temperature solid phases of nitrogen and deuterium belong. Fig. 4 shows the crystal structure of carbon dioxide represented by Model 2.

Model 3 in Fig. 3 is for acetylene HC≡CH. A cubic $Pa3$ structure with four molecules per unit cell and an orthorhombic *Pnnm* structure with two molecules per unit cell are formed by this model. The former simulates the high-temperature modification stable between −140°C and the sublimation temperature; the latter simulates, probably, the unestablished low-temperature modification below −140°C (*cf.* Figs. 11 and 12 in Part II).

Model 4 in Fig. 3 is for cyanogen N≡C–C≡N. Solid cyanogen is orthorhombic *Pbca* with a tetramolecular unit cell with the edge ratios $a/c=0{\cdot}874$ and $b/c=0{\cdot}891$. The structure given by an assembly of Model 4 is similar, with $a/c=0{\cdot}90$ and $b/c=0{\cdot}90$, as shown in Fig. 6, which is obtained by piling up the two-dimensional structure shown in Fig. 5.

1,2-dichloroethane $ClCH_2CH_2Cl$, *trans*-1,4-dibromocyclohexane

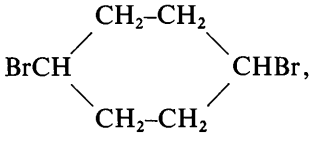

and many other quadrupolar molecules crystallize into monoclinic $P2_1/c$ with two molecules per unit cell. Model 5 is for these molecules: the structure shown in Fig. 7 simulates the real crystal structures.

Models 6–8 in Fig. 8 for disk-like quadrupolar molecules are the same as described in Parts II and III. The cubic crystal structure $Pa3$ of β-hexachlorocyclohexane $C_6H_6Cl_6$, the orthorhombic *Pbca* of solid benzene and the monoclinic $P2_1/c$ of flat molecules like naphthalene can be represented by Models 6, 7 and 8 respectively.

Octopolar and hexadecapolar molecules

Fig. 9 shows models for octopolar molecules. Models 9 and 10 are for hexamethylenetetramine and SiF_4 respectively. A body-centred cubic structure $I\bar{4}3m$ is formed by either of these models (*cf.* Fig. 2 in Part II and Fig. 13 in Part III).

Model 11 is for B_4Cl_4 or CF_4. There is an essential difference between Model 10 and Model 11 in their stable configurations of the two-molecule systems, which are compared in the same figure. Fig. 10 shows a stable two-dimensional structure into which Model 11 can be assembled. Two structures are formed by piling up this structure into layers: One gives tetragonal $P4_2/nmc$ (Fig. 11), which simulates the crystal structure of B_4Cl_4, and the other gives monoclinic $C2/c$ (Fig. 12) of α-CF_4 (Bol'shutkin, Gasan, Prokhvatilov & Erenburg, 1972).

Fig. 13 shows models for hexadecapolar molecules. Model 12 is for octa(silsesquioxane) $(HSi)_8O_{12}$ and octa(methylsilsesquioxane) $(CH_3Si)_8O_{12}$; the rhombohedral crystal structure $R\bar{3}$ of these molecules can be simulated (*cf.* Fig. 19 in Part III).

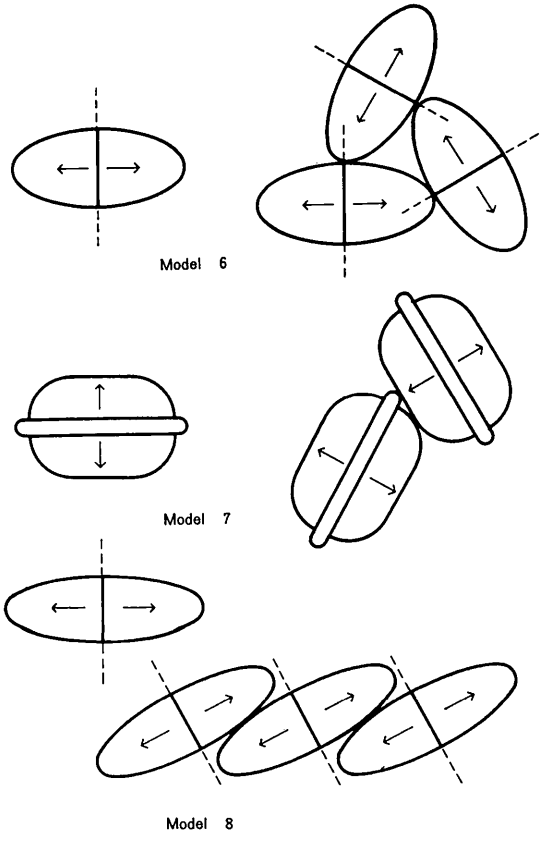

Fig. 8. Models of disk-like quadrupolar molecules and their minimum-energy configurations. Model 6 is for β-hexachlorocyclohexane $C_6H_6Cl_6$; Model 7 is for benzene C_6H_6 Model 8 is for flatter molecules like naphthalene.

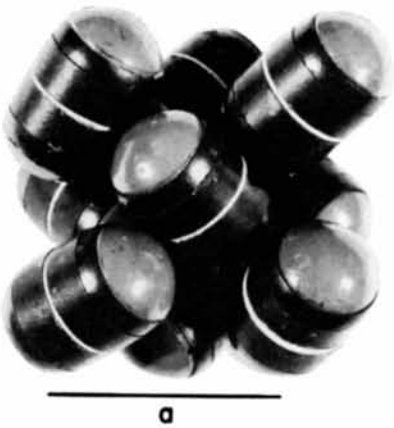

Fig. 4. Cubic *Pa*3 structure simulating the crystal structure of carbon dioxide (Model 2).

Fig. 5. A two-dimensional structure composed of Model 4.

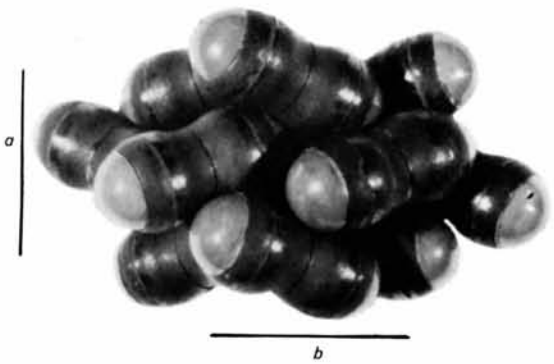

Fig. 6. Orthorhombic *Pbca* structure simulating the crystal structure of cyanogen (Model 4).

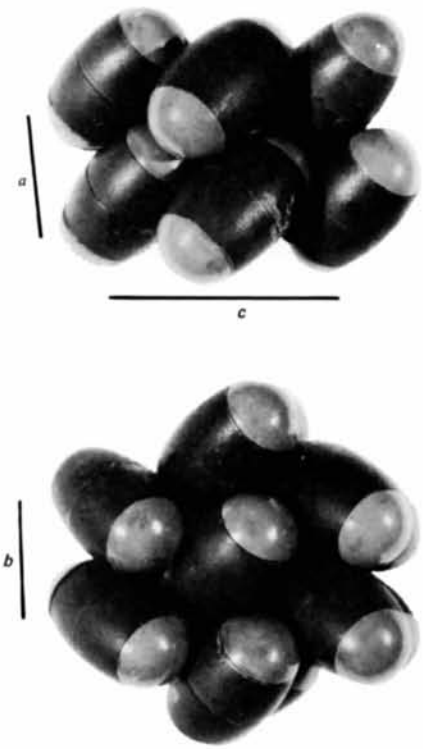

Fig. 7. Monoclinic $P2_1/c$ structure simulating the crystal structure of 1,2-dichloroethane (Model 5).

[*To face p.* 720

Fig. 10. A two-dimensional structure composed of Model 11.

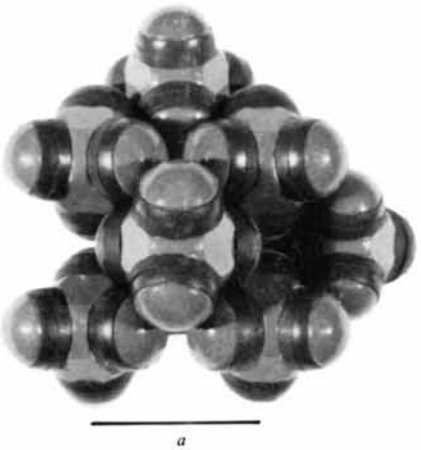

Fig. 11. Tetragonal $P4_2/nmc$ structure simulating the crystal structure of B_4Cl_4 (Model 11).

Fig. 12. Monoclinic $C2/c$ structure simulating the crystal structure of α-CF_4 (Model 11).

Fig. 14. A two-dimensional structure composed of Model 14.

Fig. 15. Rhombohedral $R\bar{3}$ structure simulating the crystal structure of WCl_6 (Model 14).

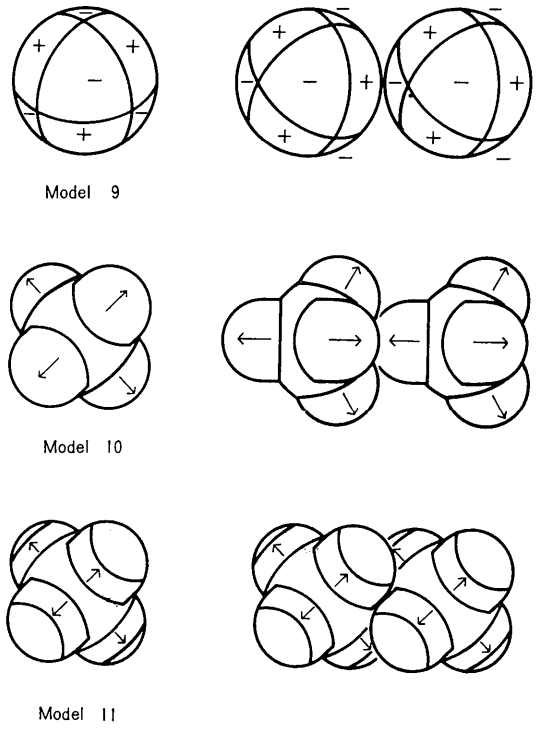

Fig. 9. Models of octopolar molecules and their minimum-energy configurations. Model 9 is for hexamethylenetetramine $(CH_2)_6N_4$; Model 10 is for SiF_4; Model 11 is for B_4Cl_4 and CF_4. Ba-ferrite magnets are with arrows; the parts without arrows are plastic or wooden pieces.

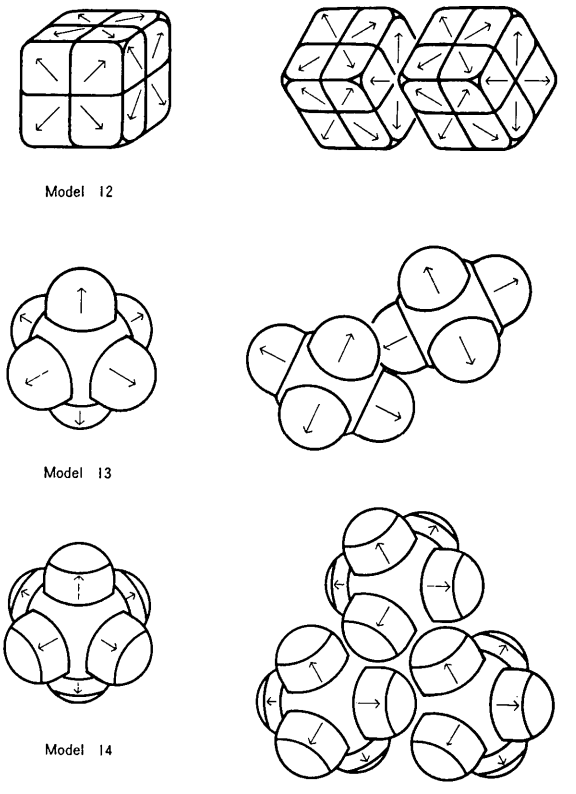

Fig. 13. Models of hexadecapolar molecules and their minimum-energy configurations. Model 12 is for $(HSi)_8O_{12}$ and $(CH_3Si)_8O_{12}$; Model 13 is for UF_6 and UCl_6; Model 14 is for WCl_6.

Model 13 is for UF_6 and UCl_6; Model 14 is for WCl_6. The multipolar interaction is very strong for UF_6 since the fluorine atom is strongly electronegative. As regards UCl_6 and WCl_6, the former is considered to have a larger hexadecapole because the ionization energy is 4 eV for uranium and 8 eV for tungsten. The two models take these differences into account; the stable configuration of the two-molecule system represented by Model 13 is compared with that of the three-molecule system represented by Model 14. By use of Model 13, both the orthorhombic *Pnma* structure for UF_6 and the trigonal $P\bar{3}m1$ structure for UCl_6 are simulated (*cf.* Fig. 21 and Fig. 20 in Part III). These crystal structures cannot be represented by Model 14, which gives rhombohedral $R\bar{3}$ formed by piling up the two-dimensional structure shown in Fig. 14 into layers as shown in Fig. 15.

Conclusion

Fourteen species of quadrupolar, octopolar and hexadecapolar molecular models explain the structures of typical molecular crystals in which electrostatic multipolar interaction plays an important part. By use of these models, some predictions can be made as regards unestablished crystal structures. The low-temperature modification of solid acetylene is probably *Pnnm* with two molecules per unit cell as represented by Model 3 (Kihara, 1966) rather than *Cmca* with four molecules per unit cell which has been inferred by some authors (Ito, Yokoyama & Suzuki, 1969; Hashimoto, Hashimoto & Isobe, 1971). The crystal structure of OsF_8 is probably $R\bar{3}$ as represented by Model 12 (Kihara, 1970); one of the high and low-temperature modifications of SF_6 is probably either *Pnma* or $P\bar{3}m1$ as represented by Model 13.

References

Bol'shutkin, N. D., Gasan, V. M., Prokhvatilov, A. I. & Erenburg, A. I. (1972). *Acta Cryst.* B**28**, 3542–3547.

Hashimoto, M., Hashimoto, M. & Isobe, T. (1971). *Bull. Chem. Soc. Japan*, **44**, 649–652.

Ito, M., Yokoyama, T. & Suzuki, M. (1969). *Spectrochim. Acta*, A**26**, 695–705.

Kihara, T. (1963). *Acta Cryst.* **16**, 1119–1123.

Kihara, T. (1966). *Acta Cryst.* **21**, 877–879.

Kihara, T. (1970). *Acta Cryst.* A**26**, 315–320.

Koide, A. & Kihara, T. (1974). *Chem. Phys.* **5**, 34–48.